

## Nucleation in the equatorial free troposphere: Favorable environments during PEM-Tropics

A. D. Clarke,<sup>1</sup> F. Eisele,<sup>2,3</sup> V. N. Kapustin,<sup>1</sup> K. Moore,<sup>1</sup> D. Tanner,<sup>2</sup> L. Mauldin,<sup>2</sup>  
M. Litchy,<sup>1</sup> B. Lienert,<sup>1</sup> M. A. Carroll,<sup>4,5</sup> and G. Albercook<sup>4</sup>

**Abstract.** A combination of aerosol and gas phase instrumentation was employed aboard the NASA-P3B as part of the Pacific Exploratory Mission-Tropics (PEM-T) in the eastern equatorial Pacific during August-October 1996. Recent particle production was found in cloud-processed air over extended regions aloft (6-8 km). These were clearly associated with clean marine air lofted by deep convection and scavenged of most aerosol mass in the Intertropical Convergence Zone (ITCZ) and in more aged cloud-scavenged air influenced by a distant continental combustion near the South Pacific Convergence Zone (SPCZ). Recent particle production was evident in regions where sulfuric acid concentrations were about  $0.5$  to  $1 \times 10^7$  molecules  $\text{cm}^{-3}$ , when surface areas were near or below  $5 \mu\text{m}^2 \text{cm}^{-3}$ , and when relative humidity (RH) was elevated over adjacent regions. In regions of recent particle production, the calculated critical sulfuric acid concentrations, based upon classical binary nucleation theory and corrected for in situ conditions near cloud, were generally consistent with nearby observed sulfuric acid concentrations. This indicates that classical binary nucleation theory and natural sources of sulfuric acid can account for nucleation in the near-cloud environment. Data from six equatorial flights between  $20^\circ\text{N}$  and  $20^\circ\text{S}$  demonstrate that this process populates extensive regions of the equatorial free troposphere with new particles. Vertical profiles suggest that nucleation, subsidence, and mixing into the MBL can supply the MBL with new aerosol.

### 1. Introduction

The origin of condensation nuclei (CN) in the remote marine atmosphere has been an objective of numerous research programs for the past 2 decades. Observations of substantial emissions of sulfur in the form of dimethylsulfide (DMS) from the ocean surface prompted suggestions that its oxidation products could provide a natural source for marine aerosol sulfate [Bonsang *et al.*, 1980; Andreae and Raemdonck, 1983]. Uncertainties over the nature of the conversion process prompted speculation that new particle formation might be initiated via gas to particle conversion and that these particles might have climatological significance through their influence on the abundance of CN and of cloud condensation nuclei (CCN) in the marine boundary layer (MBL) [Charlson *et al.*, 1987]. This interest gave rise to various experiments attempting to link DMS emissions, CN, and CCN in the MBL. However, unambiguous evidence for widespread new particle production in the MBL in response to elevated DMS has been difficult to demonstrate, although some examples exist [Hegg *et al.*, 1990; Covert *et al.*, 1992; Hoppel *et al.*, 1994]. Other

observations have indicated that condensation of gases in the MBL, for regions with typical surface areas and high DMS, was more likely to result in growth of existing aerosol to larger sizes than the formation of new particles [Clarke, 1993; Clarke *et al.*, 1996; Ayers *et al.*, 1991].

Efforts to model nucleation of new particles in the MBL have been mixed in both the assumptions used and predicted results [Shaw, 1989; Raes *et al.*, 1993; Hegg *et al.*, 1990; Russell *et al.*, 1994; Covert *et al.*, 1992]. However, it is clearly recognized that the vapor pressure of sulfuric acid and the presence of preexisting aerosol surface area are key parameters that determine whether nucleation of new particles will occur as opposed to condensation upon existing aerosol. Estimates of the maximum surface area conducive to nucleation for moderate to high sulfuric acid in the MBL suggest maximum values of about  $10 \mu\text{m}^2 \text{cm}^{-3}$ . Careful measurements of new particle production and sulfuric acid concentrations reflect these dependencies in boundary layer air influenced by local volcanic emissions [Weber *et al.*, 1995]. These measurements at Mauna Loa Observatory, Hawaii, show modest peaks in ultrafine CN concentrations of about  $60 \text{cm}^{-3}$  for surface areas below about  $10 \mu\text{m}^2 \text{cm}^{-3}$ . Typical measured MBL dry surface areas are about  $20$ - $100 \mu\text{m}^2 \text{cm}^{-3}$  [Covert *et al.*, 1996] and corresponding to about  $50$ - $200 \mu\text{m}^2 \text{cm}^{-3}$  "wet" at  $\sim 80\%$  relative humidity in the MBL. Hence, models predict that nucleation will not be favored in the MBL [Shaw, 1989; Raes, 1995] unless aerosol surface area is markedly reduced through some removal process or by incursions of air with low surface area from aloft.

Previous observations of extended high concentrations of small nuclei were made at higher altitudes in the free troposphere (FT) near regions of deep convection [Clarke, 1993], and highest concentrations were found associated with re-

<sup>1</sup>School of Ocean and Earth Science and Technology, University of Hawaii, Honolulu.

<sup>2</sup>National Center for Atmospheric Research, Boulder, Colorado.

<sup>3</sup>School of Atmospheric Sciences, Georgia Institute of Technology, Atlanta.

<sup>4</sup>Department of Chemistry, University of Michigan, Ann Arbor.

<sup>5</sup>Department of Atmospheres, Oceanic, and Space Sciences, University of Michigan, Ann Arbor.

gions of lowest aerosol mass. It was suggested that these nuclei were related to cloud processes that scavenged surface aerosol through precipitation but pumped gas phase aerosol precursors aloft [Chatfield and Crutzen, 1984] to regions where low aerosol surface area favored new particle nucleation. Other evidence for new particle formation near individual mid-latitude clouds has been observed recently [Hegg et al., 1990, Perry and Hobbs, 1994; Hoppel et al., 1994]. Nucleation consistent with these observations under similar conditions were also predicted by a FT model [Shaw, 1989; Raes et al., 1993]. Application of this model to the convective equatorial region was used to predict the evolution and growth of this aerosol during subsidence to the MBL [Raes, 1995]. The resulting predicted size distribution above the MBL was also shown to be consistent with that inferred for the observed entrainment and diurnal growth of aerosol measured in the equatorial Pacific [Clarke et al., 1996]. Extensive MBL aerosol size-distribution measurements in the Pacific have also shown that regions of high pressure tended to reveal smaller nuclei than other regions, consistent with the notion of small nuclei subsiding from above [Covert et al., 1996].

Recently, during the first Aerosol Characterization Experiment (ACE 1), observations of enhanced layers of "new" particles were found in the FT in colder mid-latitudes. These layers were generally found at altitudes (2-4 km) that corresponded to nearby cloud top heights, and focused cloud experiments demonstrated that these were recently formed particles that originated in the outflow region of clouds preferentially after late morning when photochemical processes had become sufficiently active [Clarke et al., 1998]. Extending the generality of these observations to other environments and identification of other possible conditions that might support nucleation in the remote atmosphere was one of the objectives of PEM-T.

## 2. Instrumentation

The instrumentation of relevance here include the following: (1) a condensation nuclei (CN) counter (TSI-3760) that counts total particle number for diameters from 0.011 to 3.0  $\mu\text{m}$ . A second unit operated at 300°C counts "refractory CN" (RCN) remaining after heating to 300°C (soot, dust, or sea salt); (2) an ultrafine condensation nucleus counter (UFCN) (TSI 3025) counts particles between 0.003 and 3.0  $\mu\text{m}$ ; (3) a scanning radial differential mobility analyzer (RDMA) [Zhang et al., 1995]. This device sizes particles into ~40 size bins 0.007-0.25  $\mu\text{m}$  with thermal analysis. This involves measurement at ambient temperature and then heating the aerosol to 150°C to drive off sulfuric acid and to 300°C to drive off ammonium sulfate/bisulfate so that size-resolved physical chemistry can be inferred [Clarke, 1991]; (4) a laser optical particle counter (LOPC; a modified PMS LAS-X) is used to size the larger dry aerosol (0.15-7.0  $\mu\text{m}$ ) with the same thermal analysis as the RDMA; and (5)  $\text{H}_2\text{SO}_4$ , gas phase sulfuric acid, is measured using a selected ion chemical ionization mass spectrometer instrument and inlet system [Eisele and Tanner, 1993].

The aerosol sampling system was similar to arrangements described elsewhere [Clarke, 1993; Porter et al., 1992; Clarke et al., 1996], only here we employed a shrouded isokinetic inlet nozzle on a 2-inch ID aluminum tube that was designed for an improved passing efficiency for larger aerosol sizes. Since this paper focuses on the smaller submicrometer

sizes, this difference is inconsequential. Inside the aircraft, the main inlet was followed by a flow splitter with four 12-mm pickup tubes directed flows to various sample lines. All instruments were within about 2-3 m of the splitter and were arranged such that all sample air was returned to a waste line that exhausted overboard. Hence all instruments were operated at ambient outside pressure plus about 5% overpressure due to "ram" air deceleration behind the inlet nozzle. All instruments counted continuously except for the RDMA. This drew air from an all-aluminum lagged aerosol grab (LAG) chamber [Clarke et al., 1998] that was opened every few minutes for about 15 s. Up to three size scans at three temperatures of 1 min each were completed before the LAG chamber was refilled. These RDMA scans were carried out at ambient pressure, and particle mobility was corrected for pressure at the time of sampling to ensure proper sizing at all altitudes.

The most rapid continuous aerosol measurements that characterize regions of recent nucleation are the measured differences between the UFCN counter and the CN counter or DeltaCN. Together these provide the number of particles present in the 3-11 nm range, hereafter called DCN particles. RDMA data obtained from a 15-s "grab" sample provided essential information on the changes in the size distribution between 7 and 250 nm that reveal both the presence and later evolution of these "new" nuclei. Diffusive losses at the smaller end of this size range can result in undercounting by this instrument when the size distribution is dominated by smaller particles. Diffusive losses have been characterized for the RDMA alone [Zhang et al., 1995] but not for the combined LAG chamber and RDMA thermal system as employed here. Also, the TSI 3010 detector (operated at supersaturation temperature difference of 22°C) was found to have a lower counting efficiency than expected below about 11 nm. Consequently, RDMA concentrations for sizes shown here between 7 and 11 nm are expected to underestimate actual concentrations in this range by 50% or more. Away from regions of recent nucleation and when there are few particles in this smaller size range, the total RDMA concentrations tend to underestimate total measured CN by about 20%.

## 3. ITCZ and SPCZ Free Troposphere Observations

In order to provide a framework for discussing general features of other equatorial flights (Figure 1) we will first examine the data for flight 10 (P3B) in some detail. This flight from Hawaii to Tahiti took us over the deep convection associated with the Intertropical Convergence Zone (ITCZ) and another weaker convective region in the vicinity of Tahiti (Figure 2). The latter is consistent with the boundary for the easternmost position of the South Pacific Convergence Zone (SPCZ) and will be referred to as such here. The indicated average positions (Figure 1) of the ITCZ and SPCZ during PEM-T [Fuelberg et al., this issue] are separated by a zone of gradual subsidence below 12 km altitude of about 0.5-1.0  $\text{cm s}^{-1}$  (K. Gage, personal correspondence, 1997). The SPCZ tends to be bounded by more polluted air in westerly flow on its southern side and cleaner air in easterly flow on its northern side based upon analysis of DC-8 aircraft data [Gregory et al., this issue].

A time series of flight 10 data for particle concentrations is illustrated in Figure 2a. In the marine boundary layer (MBL)

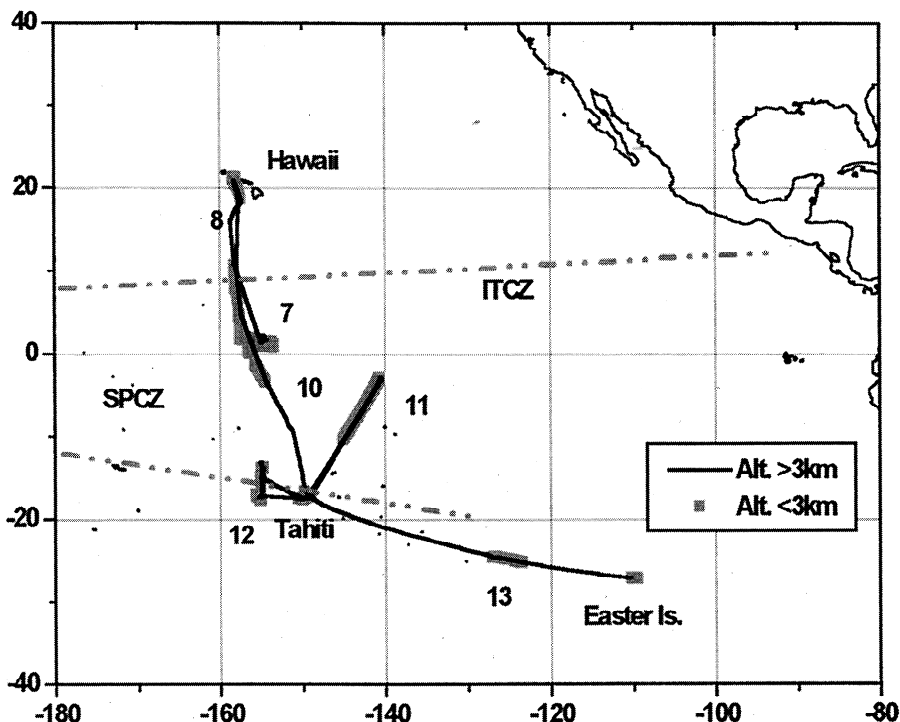


**Figure 1.** Map of flight tracks for P3B-B for missions 7, 8, 10, 11, 12, and 13 from Hawaii to Tahiti. The typical location of the ITCZ and SPCZ for the PEM-T period is indicated along with the altitude regime of the aircraft.

the UFCN and CN concentrations were similar and indicating that there are no DCN ( $3 < D_p < 11$  nm) nuclei present (within our  $\sim 5\%$  flow uncertainty for these difference measurements) at these lower altitudes. However, the DCN concentrations indicative of recent nucleation are pronounced during the high-altitude legs over the ITCZ ( $\sim 2300$ ) and also just prior to our descent into Tahiti (2830). Above the ITCZ the RCN are at the detection limit and reveal that all particles are volatile, characteristic of particles formed by gas to particle nucleation and similar to observations we have made earlier above the ITCZ [Clarke, 1993]. This is in contrast to the region to the south near Tahiti that has a similar number of CN and surface area (not shown) but where about 300 RCN remain after heating, an indication of the presence of refractory surface derived particles (soot, dust, sea salt). The absence of particles larger than  $0.6 \mu\text{m}$  in either region (not shown), as measured by the LOPC, eliminates dust and sea salt as realistic contributors to RCN and strongly suggests soot as the RCN at this altitude.

Also indicated are the concentrations of ethyne that were relatively high in the SPCZ compared to the ITCZ, along with other combustion tracers. The ratios of ethyne to carbon monoxide in these regions were about 0.3 for the ITCZ and about 1.0 for the SPCZ, suggesting air more than 10 days removed from an emission source for the ITCZ and about 5 days for the SPCZ [Gregory *et al.*, this issue]. Winds at the latter location were from the SW at about 40 m/s indicating rapid transport across the Pacific (about 2 days). This is consistent with long-range transport of polluted air high in ethyne [Gregory *et al.*, this issue], and back trajectory analysis indicates the air had come through deep convection over Africa about 6 days earlier (R. Chatfield, personal correspondence, 1998). Hence this transition in aerosol character is an indica-

tion of passing through the SPCZ into more polluted air undergoing long-range transport from the SW. Yet, in spite of these differences, new particle production is evident in both air masses.

The evidence of nucleation near ITCZ cloud features is consistent with recent observations for isolated midlatitude cloud outflow [Perry and Hobbs, 1994] and in clean marine regions near Tasmania [Clarke *et al.*, 1998]. In the latter cases, low surface area near  $5 \mu\text{m}^2\text{cm}^{-3}$  (as we measured here) and sulfuric acid exceeding  $1 \times 10^7$  molecules  $\text{cm}^{-3}$  apparently related to midday photochemical oxidation of DMS were the conditions associated with nucleation. Similar conditions and elevated sulfuric acid were characteristic for the clean ITCZ region here. However, the situation for the high DCN in the SPCZ is somewhat different. The transition to elevated RCN shown in Figure 2 near hour 27 is associated with our climbing into drier air aloft. This climb took us well above the convective clouds at about 6 km that were also characterized in the DC-8 lidar data between  $8^\circ\text{S}$  and  $12^\circ\text{S}$  taken a few hours before (E. Browell, personal correspondence, 1998). This climb was associated with a transition to air from the SW with much higher wind speeds associated with the "polluted" westerly flow already mentioned. The measured P3B ozone almost doubled on this leg after hour 28 (about  $12^\circ\text{S}$ ) indicating that we were penetrating the high ozone (60–80 ppbv) region reported for this altitude from the DC-8 DIAL lidar data [see Fuelberg *et al.*, this issue, Plate 3]. Our DCN concentrations (Figure 3) also start to increase when  $\text{O}_3$  and wind speed aboard the P3B-B increased about hour 27.8, but the highest concentrations occur later about hour 28.4 even though other pollution indicators RCN,  $\text{O}_3$ , ethyne, etc. were relatively stable. As mentioned earlier, it appears that this high-altitude "plume" originated from bio-

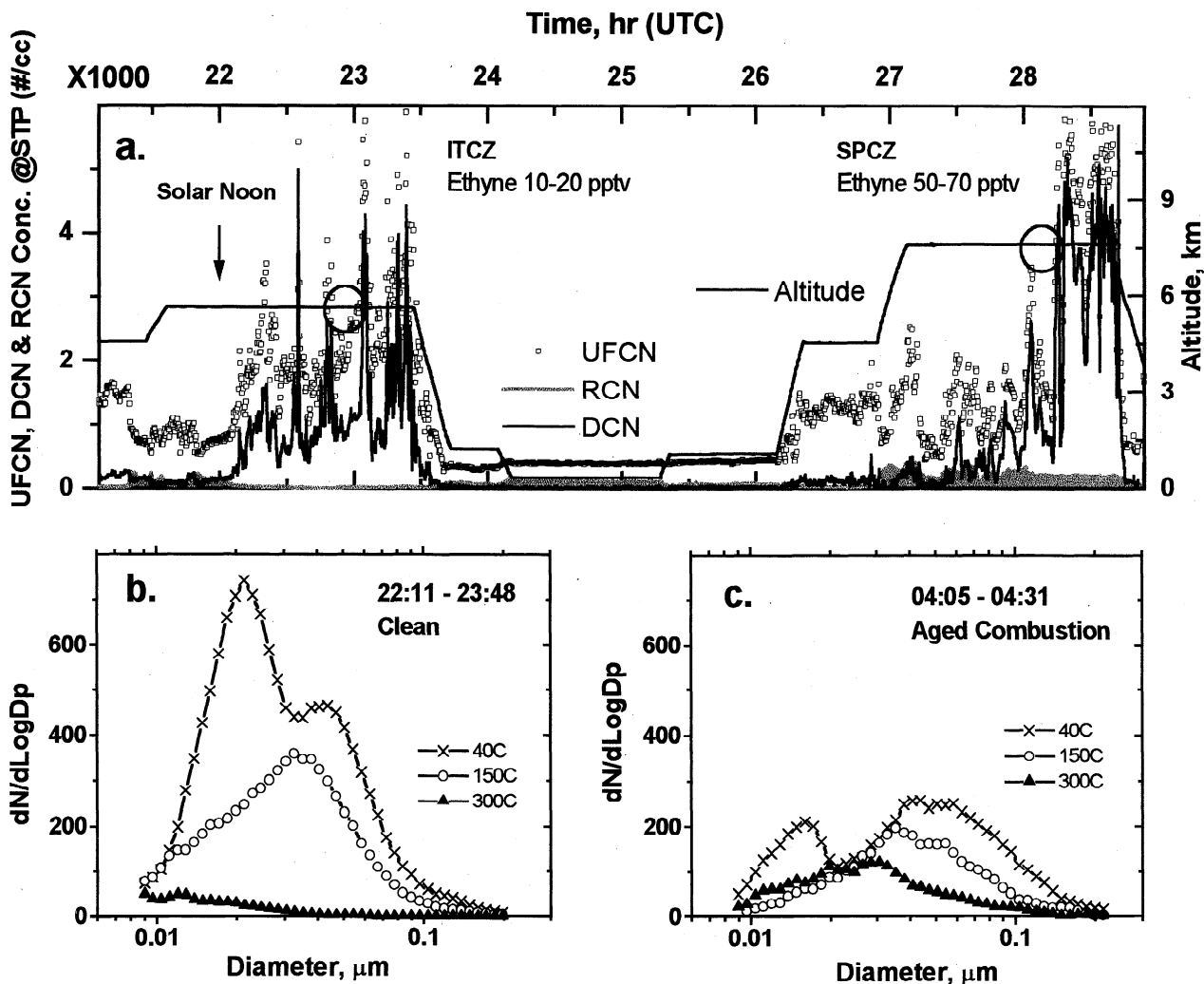


**Figure 2.** (a) Time series (continued past midnight as 25, 26, etc.) of altitude, UFCN, DCN, and RCN for flight track of P3B-B flight 10 shown in Figure 1. (b) Size distributions at the three indicated temperatures taken in the ITCZ for the circle near 2300 hours indicated in (a). (c) Same as Figure 2b, only for the SPCZ circle near 2800 hours and showing small particle peak is at smaller sizes and a refractory peak much larger, indicative of a soot core derived from combustion.

mass burning in Africa and carried aloft in deep convection. The RDMA surface areas for this leg near 9 km were fairly steady at about  $2\text{--}3 \mu\text{m}^2 \text{cm}^{-3}$  for 27–28.5 and slightly lower than the ITCZ case. These low values indicate that if this air were of combustion origin, then it had been highly scavenged of most aerosol mass earlier in its history, consistent with its original passage through precipitating clouds (R. Chatfield, personal correspondence, 1998). Unfortunately, we had no sulfuric acid data available on the P3B-B after about hour 27 because of instrument problems.

The RDMA thermally resolved size distributions from in Figures 2b and 2c reveal some fundamental differences between the elevated aerosol concentrations for the ITCZ and SPCZ cases. In Figure 2b for the clean air above the ITCZ, the unheated distribution shows a double peak with peaks at 0.02 and 0.05  $\mu\text{m}$ . After heating to 150°C, the smaller peak has volatilized, and the larger peak has shifted slightly smaller. This suggests the smaller peak was primarily sulfuric acid while the larger aerosol included a more ammoniated aerosol [Clarke, 1991]. Further heating to 300°C is seen to remove most of the remaining aerosol number, suggesting this

component has an ammonium sulfate/bisulfate composition and that most were formed in situ by gas to particle conversion. The difference in volatility reveals a difference in chemical composition for these two modes that shows that they coexist as external mixtures and were formed separately, with the smaller sulfuric acid peak formed later in the presence of the ammonium bisulfate peak. The latter appears to have been partially neutralized previously, because if ammonia gas were present when the smaller peak were formed, we would have expected it to also have been partially neutralized.

A thermally resolved RDMA size distribution for the SPCZ long-range transport “pollution” mode differs in several ways (Figure 2c). It is also “bimodal” and is again associated with a small peak volatile at 150°C but has a smaller diameter. The larger peak is at a slightly greater diameter than the ITCZ case and has more volatile sulfuric acid associated with it. The most significant difference is seen for the 300°C distribution. Unlike the ITCZ case, the refractory distribution is only shifted to slightly smaller sizes than the 150°C peak, and the total number at 300°C (integrated area under the curve) is only slightly less. This indicates that, unlike the ITCZ aero-

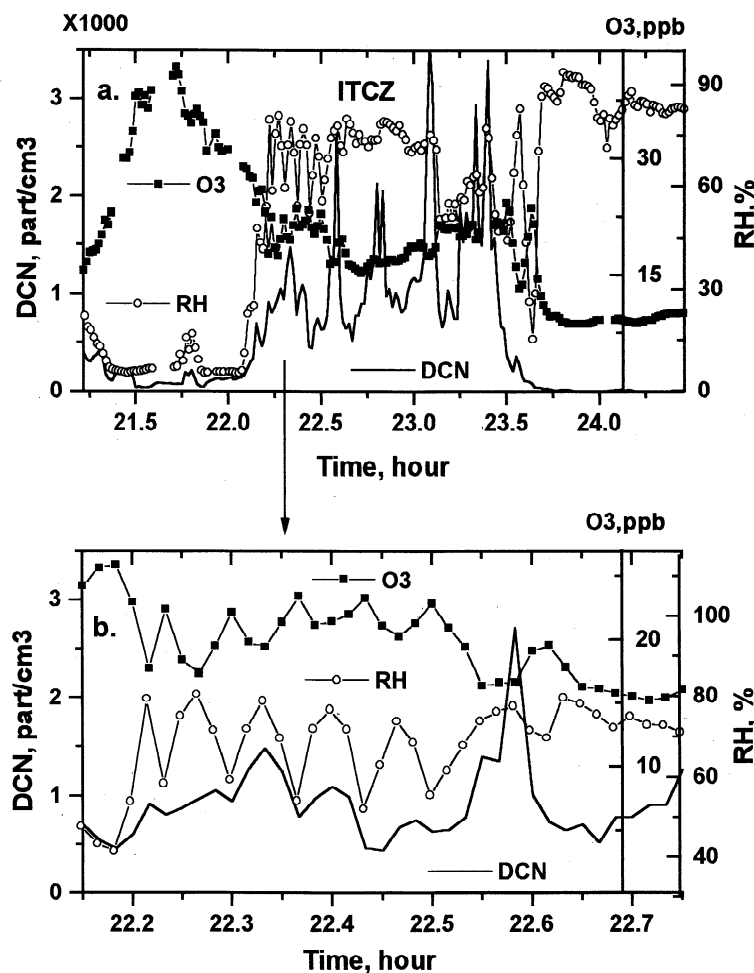


**Figure 3.** (a) Expanded time series (Figure 2; 2130–2400) for altitude, DCN (UFCN-CN) and RH and ozone for ITCZ region in flight 10. (b) Further expanded time series for northernmost half of ITCZ region showing clear coupling between DCN, ozone, and RH as a result of cloud processes.

sol, a large fraction of the number originated as a primary emission of refractory aerosol (RCN) at the Earth's surface that has added volatile mass through heterogeneous gas to particle conversion (GPC) over time. The properties and size of these RCN are most consistent with them having a sootlike core. This characteristic has been observed in pollution aerosol over the Atlantic that originated from central Europe [Clarke *et al.*, 1996]. However, in spite of high pollutant concentrations and associated gaseous precursors, we found no evidence for nucleation in the polluted Atlantic, presumably suppressed by the high surface area present. Again, the volatility difference for the two nuclei modes shown in Figures 2b and 2c suggests that homogeneous nucleation of new nuclei is also responsible for the formation of the smaller diameter mode in the presence of the residual aged combustion aerosol that dominates the larger mode. This inference is again supported by the measurements of high levels of ozone and ethyne in this region. These observations suggest that nucleation can occur in aged polluted air provided it has been scavenged of most surface area.

#### 4. Cloud Outflow

In order to demonstrate the relationship of cloud outflow to new particle production we have expanded the time period for the flight leg above the ITCZ and subsequent descent in Fig-

ure 3. For the initial part of the leg at 6 km (Figure 3a) the air is dry with RH of 10% and has high ozone indicative of stratospheric air. Just after 21.75 hours the DCN increase slightly at the same time that RH increases, and ozone drops for about 5 min (30 km), suggesting the influence of cloud-pumped air. The recently formed DCN increase significantly near 22.0 hours and remain broadly elevated over the ITCZ for over 500 km at nearly  $1000 \text{ cm}^{-3}$  and with isolated maxima of several thousand per  $\text{cm}^3$ . Above the ITCZ, ozone goes through a relative minimum centered on this region at 1020 min, and RH is elevated. These all indicate that the region is influenced by air pumped from below that has low ozone and high water vapor. The detailed structure of ozone and RH over this region is shown on a further expanded scale in Figure 3b. Both are clearly anticorrelated with peak widths that correspond to regions about 20–60 km across and on the scale of individual cumulus tower tops. The DCN structure superimposed on the broad elevated DCN concentrations in this region (Figure 3b) also correspond to the elevated RH values and ozone minima, indicating all features relate to cloud outflow. The relative magnitudes of the DCN peaks are variable (Figure 3a), as expected, since the particle concentrations detected will depend upon many parameters such as their size, the time for evolution since being produced, the actinic flux (photochemistry), cloud processes, precursor source strengths, etc. Even so, the particle concentrations and their

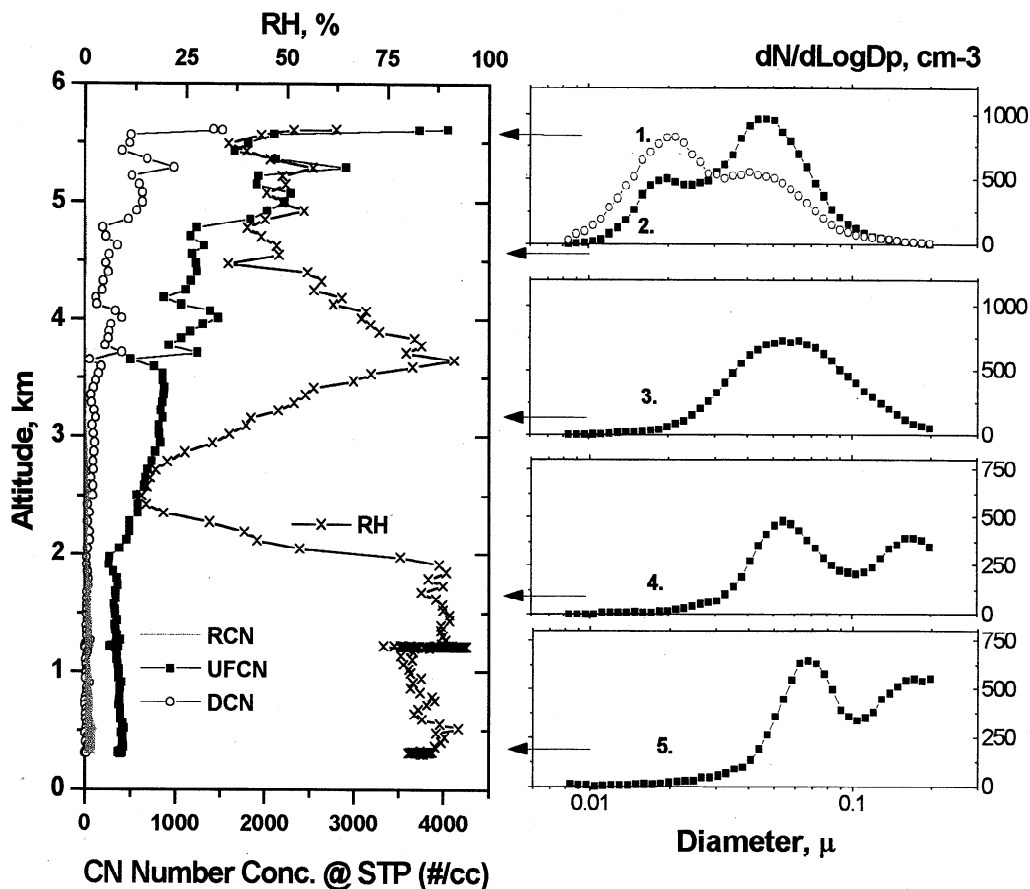


**Figure 4.** (left) Vertical profile south of ITCZ for UFCN, DCN and RCN. Panels indicate RDMA number distributions and associated altitudes during profile.

spatial scales are clearly related to pulses of cloud-processed air at these altitudes.

A vertical profile (Figure 4a) made about 23.5 hours (Figure 2a) south of the ITCZ descends through a region of recent nucleation. DCN and CN concentrations are highest aloft near the ITCZ and decrease toward the surface where the aerosol appears well mixed below 2 km. CN concentrations are constant at a few hundred per cm<sup>3</sup> in the MBL, and no significant DCN are present in the MBL. RCN are negligible aloft, as expected for nuclei formed in situ, and increase to about 30 cm<sup>-3</sup> in the MBL, largely due to sea salt. RH is high in the MBL but dry above in the subsidence inversion near 2 km. The increase in RH above that altitude is associated with a strong decrease in ozone (see Figure 3a after 23.5 hours). Ozone and RH are anticorrelated throughout the descent and indicate that the dry troposphere has been moistened aloft through ITCZ cloud pumping. The elevated concentrations of new particles are associated with this regional cloud outflow as it spreads away from the ITCZ in a layer more than 3 km deep.

The gradient in nuclei from aloft toward the surface is also linked to changes in the RDMA size distribution measured during descent and shown in Figure 4b for five representative altitudes indicated by arrows. The dry free troposphere (FT) air near 2.5 km does not appear recently perturbed by cloud outflow, and the well aged number distribution 3 is broad and monomodal centered near 0.05 μm. The two distributions 1 and 2 above this altitude include both this mode and an additional smaller mode superposed at diameters near 0.02 μm.

This smaller mode 1 near 5.5 km is consistent with recent observations of photochemical production of nuclei in midlatitude cloud outflow during the day but for lower cloud tops [Clarke *et al.*, 1998]. In the next lower panel the mode amplitude is smaller and is shifted to somewhat larger sizes that appear to contribute to the larger preexisting mode. This gradient in concentration and apparent growth on descent is likely to be a climatological feature since it is present in similar profiles made in 1990 [Clarke, 1993] and about a year earlier near Christmas Island [Clarke *et al.*, 1998]. These also revealed a monomodal aerosol at intermediate altitudes that appeared to be replenished and maintained by the formation and evolution of smaller nuclei that grow and sustain this mode.

The lower two panels (1.6 km and 0.8 km) are distributions in the upper and lower regions of the MBL. These show lower particle concentrations than aloft, particularly at smaller diameters ( $D_p < 0.03$  μm), and a shift in the FT mode near 0.05 μm to larger diameters near 0.06 μm. There is also an increase in concentrations in the larger sizes near 0.15 μm and the presence of a relative minima near 0.1 μm. All of these characteristics are consistent with a monomodal aerosol entrained into MBL followed by cloud processes that activate the larger aerosol and favor their growth. This occurs through a relative increase in heterogeneous GPC due to their greatly enhanced surface area in-cloud that, upon evaporation of the cloud, results in the formation of a minimum [Hoppel *et al.*, 1994] near or below 0.1 μm. This process in the equatorial region was recently characterized through surface measurements on

nearby Christmas Island (2°N, 157°W) [Clarke *et al.*, 1996], and the distributions inferred in that paper for the FT aerosol size distributions are confirmed by this measured size distribution at 3 km. The larger of these nuclei that mix into the MBL will activate in cloud and grow to accumulate most of the aerosol mass, usually in the form of sulfate.

## 5. Discussion

Both clean and pollution cases shown in Figure 2 suggest that recent homogeneous nucleation is responsible for forming the smaller mode and that condensation is adding mass to the larger mode. However, the integral number concentrations obtained for these RDMA distributions are of the order half of the measured CN and much less of the total (Figure 2a). Some of this undercounting of CN is due to diffusive loss terms of the smaller aerosol measured by the RDMA due to the sampling system and because the RDMA does not count the particles larger than 0.25  $\mu\text{m}$ . However, the much higher UFCN than CN indicates the presence of high concentrations of DCN particles that are too small to be sized by the DMA and which would appear as a much smaller mode between 0.003 and 0.01  $\mu\text{m}$ . This suggests that nucleation may be ongoing in both "clean" and "polluted" regions, and the small mode discussed above may have formed perhaps during the prior day and is growing larger in the presence of the nucleation of new particles. This would be in agreement with the calculated time to grow to the 0.02 diameter peak seen for the ITCZ data (Figure 2b), estimated to be about 30 hours based upon the approach used by Hoppel *et al.* [1994] for an accommodation coefficient of 0.7 (determined in free troposphere on PEM-T, Doug Davis, personal correspondence, 1998) and sulfuric acid concentration of  $1 \times 10^7$  molecules  $\text{cm}^{-3}$ . Similarly, the time to grow to the 3-nm UFCN detection limit would be about 5 hours. Even so, the integral DMA number concentrations under these conditions (e.g., Figures 2a and 2b) are about a factor of 2 less than the actual CN concentrations. Since RDMA concentrations are only about 20% lower during other periods, this also suggests greater losses than expected in the smallest RDMA sizes.

A greater sense of the large-scale aerosol dynamics for the different regions and altitudes experienced on flight 10 is illustrated in Figure 5. Here a continuous series of RDMA size distributions is shown in a 3-D plot with projected altitude included for reference. These distributions describe the behavior of the aerosol number distribution and do not directly reflect behavior of surface area or mass. The sequence follows transitions from Hawaii to above the ITCZ, dropping down to near the ocean surface in the divergent easterlies and then climbing above the SPCZ before descending to Tahiti. Regions at altitude but away from the ITCZ and SPCZ generally show a monomodal aerosol with number peaks near 0.03 to 0.05  $\mu\text{m}$  with somewhat larger sizes and concentrations in the aged pollution aerosol near the SPCZ, as mentioned earlier.

A shift to larger sizes during descent between the ITCZ and SPCZ is clear along with the development of the "Hoppel" minimum associated with distributions in the MBL due to cloud processing. As mentioned earlier, less than 20% of the MBL number is RCN from sea salt as evident on descent into the MBL near 24 hours (Figure 2). These RCN represent a small fraction of the number in the large mode above 0.1  $\mu\text{m}$  seen in the MBL in Figure 5. This is consistent with previous MBL measurements in this region that show this larger

mode being primarily a natural sulfate aerosol [Clarke *et al.*, 1987] that has added mass heterogeneously after subsidence into the MBL [Clarke *et al.*, 1996] as a result of processing through low level nonprecipitating MBL clouds. It is also clear that concentrations of particles larger than about 0.06  $\mu\text{m}$  are very low for the upper level ITCZ outflow from deep precipitating cumulus with their roots in the MBL. This demonstrates that most MBL aerosol activated in these clouds are efficiently scavenged before the cloud processed air detrains and mixed near cloud top. It is this scavenging of the MBL air that drops the aerosol surface area and vents reactive gases aloft into cold air that favors the observed nucleation in these regions [Clarke *et al.*, 1998]. This demonstrates that MBL aerosol mass carried toward the ITCZ is effectively removed by this deep convection, but that aerosol number is actually increased through the production of new nuclei aloft in this cloud processed air.

These observations further support the notion that the MBL CN concentrations in clean marine regions can be maintained by aerosol nucleation in the FT associated with cloud outflow [Clarke, 1993; Perry and Hobbs, 1994] that subside, evolve, and entrain into the MBL [Shaw, 1989; Raes, 1995; Clarke *et al.*, 1996; Raes *et al.*, 1993]. However, it must be recognized that the aerosol evolution during subsidence and mixing suggested by Figure 4 does not occur directly in the column through which we descended. Subsidence velocities below 8 km estimated from wind profiler data on Christmas Island (K. Gage, personal correspondence, 1997) agree with entrainment estimates into the MBL [Clarke *et al.*, 1996] of about 0.5  $\text{cm s}^{-1}$  (430  $\text{m d}^{-1}$ ). Hence particles produced near 5 km require a week to reach the inversion at 2 km. Clearly, those produced near Christmas Island will be advected away. However, the winds blowing parallel to the ITCZ for many days provide opportunities for similarly produce particles from other ITCZ regions to undergo the subsidence suggested by the Figure 4 profile. The fact that we have observed similar profiles near Tahiti in 1990 [Clarke, 1993] and Christmas Island in 1995 [Clarke *et al.*, 1998] supports the generality of

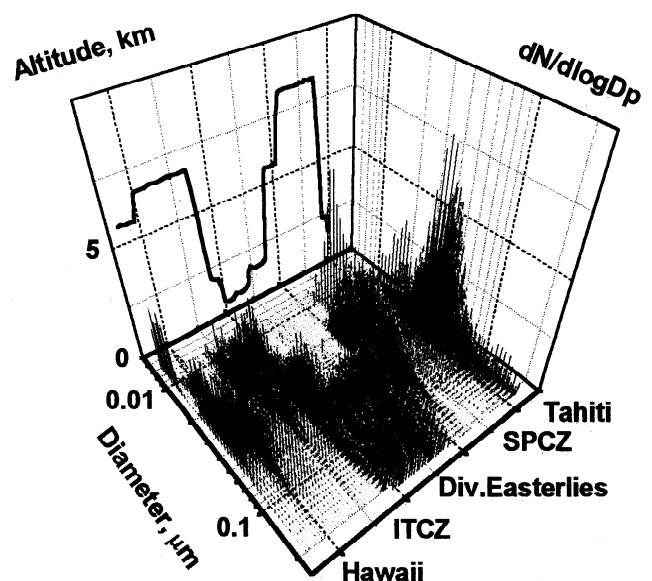
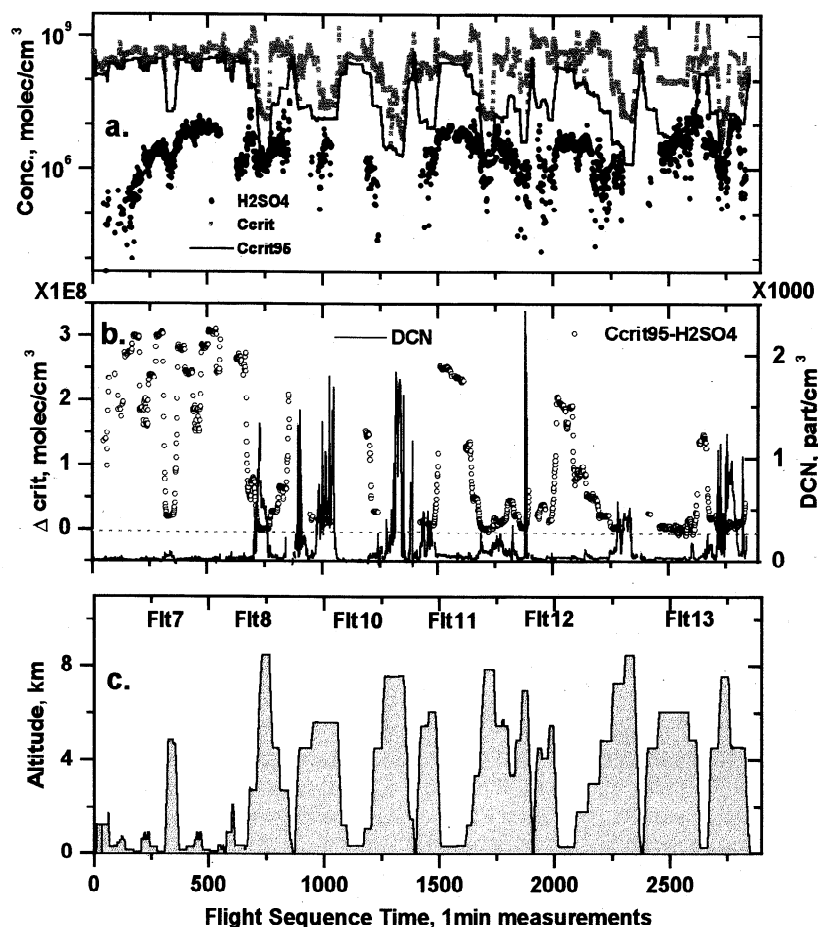


Figure 5. Sequential size distributions and projected altitudes for all RDMA distributions measured on flight 10 showing regional and altitude dependent characteristics.



**Figure 6.** A time series expressed in contiguous minutes for flights shown in Figure 1 showing (a) H<sub>2</sub>SO<sub>4</sub> measured, critical sulfuric acid content C<sub>crit</sub> at ambient RH and at 95% RH; (b) DCN (ultrafine) concentrations and DeltaCrit (H<sub>2</sub>SO<sub>4</sub> – C<sub>crit</sub>95); (c) altitudes.

these observations and the notion of nuclei evolution during subsidence. The increase in size and decrease in concentrations (Figure 4) of the aerosol during subsidence still result in concentrations above the MBL that are higher than in the MBL. Hence the effect of subsidence and entrainment into the MBL will increase MBL particle number, as needed to maintain observed stable concentrations in the MBL against typical removal processes.

It is of interest to ask whether this evidence for nucleation in cloud outflow is consistent with classical binary nucleation theory. To address this we combine all of the PEM-T flights shown in Figure 1 for this equatorial region. These are assembled as a sequential concatenated time series in Figure 6. In order to relate gas phase observations of sulfuric acid (Figure 6a) to observations of new particles (DCN) on these flights (Figure 6b), it is instructive to employ the concept of a critical sulfuric acid concentration, C<sub>crit</sub>. This is the sulfuric acid concentration required at a given RH and temperature T if a nominal nucleation rate of 1 cm<sup>-3</sup> s<sup>-1</sup> is to be achieved, and it is based upon approximation to classical binary nucleation of sulfuric acid and water. We use the formula below [Wexler *et al.*, 1994], where RH ranges from 0 to 1 and T is in kelvins, but with the conversion factor of 6.1 × 10<sup>9</sup> to yield molecules per cm<sup>3</sup>:

$$C_{\text{crit}} = 0.16 \exp(0.1 T - 3.5 \text{RH} - 27.7) \quad (\mu\text{g m}^{-3})$$

In regions where nucleation is evident and intermittent and where sulfuric acid is the likely source, it is reasonable to ex-

pect that the highest observed concentrations of sulfuric acid should at times approach critical values for nucleation. Similarly, when DCN are high and recent nucleation is most evident, we might expect that sulfuric acid could be consumed more rapidly and reduce concentrations to lower values. Hence high sulfuric acid and high DCN would not be expected to occur simultaneously, but we should expect statistically that peaks in both should be present in regions of nucleation. Figure 6b shows the periods of elevated DCN are frequently present at higher altitudes (Figure 6c) for the five flights shown in Figure 1. Sulfuric acid concentrations are shown in Figure 6a along with C<sub>crit</sub> calculated for measured ambient RH and temperature. Although C<sub>crit</sub> is lowest for the altitude legs of highest DCN concentrations, the measured sulfuric acid concentrations are about a factor of 4 to 10 below the C<sub>crit</sub> expected for classical nucleation theory.

However, it is important to realize that the smallest particles that can be detected with our UFCN instrumentation are about 3 nm diameter and much larger than the initial nuclei formed during the onset of nucleation. Hence nucleation has already occurred before it is evident in the DCN data. Consequently, if nucleation occurs in cloud outflow, then during subsequent mixing with the dry FT air the RH will continually drop. This suggests that the appropriate C<sub>crit</sub> to compare with measured sulfuric acid should be for high RH closest to the cloud outflow region. We assume here that the temperature is about the same as for the cloud outflow region. If we define a C<sub>crit</sub>95 at the measured ambient temperature but at 95% RH

expected near cloud outflow, then we can compare  $C_{\text{crit}95}$  to sulfuric acid concentrations. Figure 6a shows the values of  $C_{\text{crit}95}$ , and it is clear that measured sulfuric acid concentrations (not corrected here for dilution effects subsequent to being in the 95% RH environment) equal or approach  $C_{\text{crit}95}$  in most regions of elevated DCN. This suggests that classical binary nucleation may be adequate to describe nucleation for those locations where we see high DCN, provided nucleation occurred in the immediate vicinity of cloud edges (RH=95%).

This is more evident if the difference between sulfuric acid and  $C_{\text{crit}95}$ , DeltaCrit, is plotted in Figure 6b along with DCN. When the difference is near zero then nucleation is most likely and in most cases this is when nucleation was observed. However, a clear exception is evident near 2500 min. This can be understood when we remember that the use of  $C_{\text{crit}95}$  is based upon the assumption that it can describe the enhanced probability of nucleation in air recently processed through cloud outflow. However, not all air has recently been processed through cloud outflow. In fact, the period around 2500 min (flight 13) had very dry air, as evident in the large difference in  $C_{\text{crit}}$  and  $C_{\text{crit}95}$  (Figure 6a), and had very high ozone indicative of a stratospheric source. The 200-mb global wind divergence map for this day (R. Newell, PEM-Tropics, MIT Data Memo 6b, 1997) also shows this location to be one of the most active convergence regions (subsidence). Hence, this is not recent cloud-processed air, and the moderate sulfuric acid appears to have another source that is linked to dry air aloft that did not have a recent RH history conducive to nucleation. In most other instances the use of DeltaCrit appears consistent with elevated DCN for these flights between 20°N and 20°S. This tends to confirm the notion of cloud-processed air as a source of new particle production in the FT and that classical binary nucleation of sulfuric acid and water can be applied to the phenomena. Even so, the possibility of enhanced ternary nucleation due to the presence of low concentrations of ammonia [Coffman and Hegg, 1995; Weber et al., 1998] cannot be ruled out.

Moreover, these elevated DCN were observed during most high-altitude legs and for several hundred kilometers at a time. This confirms earlier suggestions [Clarke, 1993; Raes et al., 1993] that the ITCZ and SPCZ can generate extensive veils of new nuclei that can spread aloft, grow, and contribute to the FT aerosol. Through subsidence, this can later "seed" the MBL by providing centers for subsequent heterogeneous growth.

## 6. Summary

We have described large-scale environments where nucleation of new particles were observed in the remote tropical troposphere during PEM-T and linked them to sulfuric acid chemistry and meteorological process that are involved. Nucleation observed near the ITCZ confirms that cloud outflow provides a major source region for new particle production in the free troposphere. This includes nucleation in aged air aloft undergoing long-range transport with characteristics suggestive of combustion origins and also in well scavenged near-surface air over productive waters with high DMS. In all cases, surface areas were near or below  $5 \mu\text{m}^2 \text{cm}^{-3}$  while sulfuric acid was elevated and about  $0.5\text{--}1 \times 10^7 \text{ molecule cm}^{-3}$ . Humidity and water vapor concentrations were variable but were relatively enhanced in all regions where nucleation was evident. The variability in RH and its relationship to recent nucleation confirm the role of RH in this process [Perry and

Hobbs, 1994] and that the fluctuations in RH or water vapor concentration are important [Kerminen and Wexler, 1994]. Classical binary nucleation theory for sulfuric acid and water in this environment under the assumption that it occurred at 95% RH in the vicinity of clouds was shown to be consistent with periods of enhanced nucleation. Taken together, these observations indicate that, regardless of the source of precursor gases (natural marine emissions or long-range transport of combustion products), nucleation appears common in clean cloud-scavenged regions of the remote atmosphere (surface areas reduced below about  $5 \mu\text{m}^2 \text{cm}^{-3}$ ). The repeated observations and extensive spatial scales indicate that this is a major mechanism for sustaining the aerosol number concentration in the tropical free troposphere.

**Acknowledgments.** This research was sponsored by the NASA Tropospheric Chemistry Program under grant NAG 1 1764. We particularly appreciate the support of Joe McNeal, Jim Hoell, and the GTE Project Office. A special thanks is also extended to the people of the Wallops Island facility and the P3B-B aircraft for their repeated assistance in accommodating our needs throughout the experiment. SOEST contribution no. 4676.

## References

- Andreae, M. O., and H. Raemdonck, Dimethyl sulfide in the surface ocean and marine atmosphere: A global view, *Science*, **2**, 744-747, 1983.
- Ayers, G. P., J. P. Ivey, and R. W. Gillet, Coherence between seasonal cycles of dimethylsulfide, methanesulfonate, and sulfate in marine air, *Nature*, **349**, 404-406, 1991.
- Bates, T. S., R. P. Kiene, G. V. Wolfe, P. A. Matrai, F. P. Chavez, K. R. Buck, B. W. Blomquist, and R. L. Cuhel, The cycling of sulfur in surface seawater of the northeast Pacific, *J. Geophys. Res.*, **99**, 7,835-7,843, 1994.
- Bonsang, B., B. C. Nguyen, A. Gaudry and G. Lambert, Sulfate enrichment in marine aerosols owing to biogenic gaseous sulfur compounds, *J. Geophys. Res.*, **85**, 7410-7416, 1980.
- Charlson, R. J., J. E. Lovelock, M. O. Andreae, and S. G. Warren, Oceanic phytoplankton, atmospheric sulfur, cloud albedo, and climate, *Nature*, **326**, 655-661, 1987.
- Charlson, R. J., S. E. Schwartz, J. M. Hales, R. D. Cess, J. A. Coakely Jr., J. E. Hansen, and D. J. Hofmann, Climate forcing by anthropogenic aerosols, *Science*, **255**, 423-430, 1992.
- Chatfield, R., and P. Crutzen, Sulfur dioxide in remote oceanic air: Cloud transport of reactive precursors, *J. Geophys. Res.*, **89**, 7111-7132, 1984.
- Clarke, A. D., A thermo-optic technique for in-situ analysis of size resolved aerosol physicochemistry, *Atmos. Environ., Part A*, **25**, 635-644, 1991.
- Clarke, A. D., Atmospheric nuclei in the Pacific midtroposphere: Their nature, concentration, and evolution, *J. Geophys. Res.*, **98**, 20,633-20,647, 1993.
- Clarke, A. D., N. C. Ahlquist, and D. S. Covert, The Pacific marine aerosol: Evidence for natural acid sulfates, *J. Geophys. Res.*, **92**, 4179-4190, 1987.
- Clarke, A. D., Z. Li, and M. Litchy, Aerosol dynamics in the equatorial Pacific marine boundary layer: Microphysics, diurnal cycles and entrainment, *Geophys. Res. Lett.*, **23**, 733-736, 1996.
- Clarke, A. D., T. Uehara, and J. N. Porter, Lagrangian evolution of an aerosol column during the Atlantic stratocumulus transition experiment, *J. Geophys. Res.*, **101**, 4351-4362, 1996.
- Clarke, A. D., J. L. Varner, F. Eisele, R. Tanner, L. Mauldin, and M. Litchy, Particle production in the remote marine atmosphere: Cloud outflow and subsidence during ACE 1, *J. Geophys. Res.*, **103**, 16,397-16,409, 1998.
- Coffman, D., and D. Hegg, The effect of ammonia on particle nucleation, *J. Geophys. Res.*, **100**, 7147-7160, 1995.
- Covert, D. S., V. N. Kapustin, P. K. Quinn, and T. S. Bates, New particle formation in the marine boundary layer, *J. Geophys. Res.*, **97**, 20,581-20,589, 1992.
- Covert, D. S., V. N. Kapustin, T. S. Bates, and P. K. Quinn, Physical properties of marine boundary layer aerosol particles of the mid-

- Pacific in relation to sources and meteorological transport, *J. Geophys. Res.*, **101**, 6919-6930, 1996.
- Eisele, F. L., and D. J. Tanner, Measurement of the gas phase concentration of H<sub>2</sub>SO<sub>4</sub> and methane sulfonic acid and estimates of H<sub>2</sub>SO<sub>4</sub> production and loss in the atmosphere, *J. Geophys. Res.*, **98**, 9001-9010, 1993.
- Fuelberg, H. E., R. E. Newell, D. P. Longmore, Y. Zhu, D. J. Westberg, and E. V. Browell, A meteorological overview of the PEM-Tropics period, *J. Geophys. Res.*, this issue.
- Gregory, G. L., et al., Chemical characteristics of Pacific tropospheric air in the region of the ITCZ and SPCZ, *J. Geophys. Res.*, this issue.
- Hegg, D. A., L. F. Radke, and P. V. Hobbs, Particle production associated with marine clouds, *J. Geophys. Res.*, **95**, 13,917-13,926, 1990.
- Hoppel, W. A., G. M. Frick, and R. E. Larson, Effect of non-precipitating clouds on the aerosol size distribution in the marine boundary layer, *Geophys. Res. Lett.*, **13**, 125-128, 1986.
- Hoppel, W. A., G. M. Frick, J. W. Fitzgerald, and R. E. Larson, Marine boundary layer measurements of new particle formation and the effects nonprecipitating clouds have on aerosol size distributions, *J. Geophys. Res.*, **99**, 14,443-14,459, 1994.
- Kerminen, V.-M., and A. S. Wexler, Particle formation due to SO<sub>2</sub> oxidation and high relative humidity in the marine boundary layer, *J. Geophys. Res.*, **99**, 25,607-25,614, 1994.
- Mirabel, P., and J. L. Katz, Binary homogeneous nucleation as a mechanism for the formation of aerosols, *J. Chem. Phys.*, **60**, 1138-1144, 1974.
- Perry, K. D., and P. V. Hobbs, Further evidence for particle nucleation in clear air adjacent to marine cumulus clouds, *J. Geophys. Res.*, **99**, 22,803-22,818, 1994.
- Porter, J. N., A. D. Clarke, G. Ferry, and R. F. Penschel, Aircraft studies of size-dependent sampling through inlets, *J. Geophys. Res.*, **97**, 3815-3824, 1992.
- Raes, F., Entrainment of free-tropospheric aerosol as a regulating mechanism for cloud condensation nuclei in the remote marine boundary layer, *J. Geophys. Res.*, **100**, 2893-2903, 1995.
- Raes, F., R. Van Dingenen, J. Wilson, and A. Saltelli, Cloud condensation nuclei from dimethylsulfide in the natural marine boundary layer: remote vs. in-situ production, in *Dimethylsulfide, Ocean, Atmosphere and Climate*, edited by G. Restelli and G. Angeletti, pp. 311-322, Kluwer Acad., Norwell, Mass, 1993.
- Russell, L. M., S. N. Pandis, and J. H. Seinfeld, Aerosol production and growth in the marine boundary layer, *J. Geophys. Res.*, **99**, 20,989-21,004, 1994.
- Shaw, G. E., Production of condensation nuclei in clean air by nucleation of H<sub>2</sub>SO<sub>4</sub>, *Atmos. Environ.*, **23**, 2053-2057, 1989.
- Weber, R. J., P. H. McMurray, F. L. Eisele, and D. J. Tanner, Measurement of expected nucleation precursor species and 3-500 nm diameter particles at Mauna Loa Observatory, Hawaii, *J. Atmos. Sci.*, **52**, 2242-2257, 1995.
- Weber, R. J., P. H. McMurry, L. Mauldin, D. Tanner, F. Eisele, F. Brechtel, S. Kreidenweis, G. Kok, R. Schillawski, and D. Baumgardner, A study of new particle formation and growth involving biogenic trace gas species measured during ACE 1, *J. Geophys. Res.*, **103**, 16,385-16,396, 1998.
- Wexler, A. S., F. W. Lurmann, and J. H. Seinfeld, Modeling urban and regional aerosols, 1, Model development, *Atmos. Environ.*, **28**, 531-546, 1994.
- Zhang, S. H., Y. Akutsu, L. M. Russell, R. C. Flagan, and J. H. Seinfeld, Radial differential mobility analyzer, *Aerosol Sci. Technol.*, **23**, 357-371, 1995.

---

G. Albercook and M. A. Carroll, Department of Chemistry, University of Michigan, Ann Arbor, MI 48109-2143.

A. D. Clarke, V. N. Kapustin, B. Lienert, M. Litchy, and K. Moore, School of Ocean and Earth Science and Technology, University of Hawaii, Honolulu, HI 96822.  
(e-mail: tclarke@soest.hawaii.edu)

F. Eisele, L. Mauldin, and R. Tanner, National Center for Atmospheric Research, Boulder, CO 80303.

(Received October 16, 1997; revised June 12, 1998; accepted June 20, 1998.)